Phytochemistry 154 (2018) 10–18

Contents lists available at ScienceDirect

Phytochemistry

journal homepage: www.elsevier.com/locate/phytochem

# Structural and biosynthetic studies on eremophilenols related to the phytoalexin capsidiol, produced by *Botrytis cinerea*

Ivonne Suárez[a], Gesiane da Silva Lima[a], Raphael Conti[a,c], Cristina Pinedo[a], Javier Moraga[a], Javier Barúa[a], Ana Ligia L. de Oliveira[a,c], Josefina Aleu[a], Rosa Durán-Patrón[a], Antonio J. Macías-Sánchez[a], James R. Hanson[b], Mônica Tallarico Pupo[c], Rosario Hernández-Galán[a], Isidro G. Collado[a,*]

[a] Departamento de Química Orgánica, Facultad de Ciencias, Campus Universitario Río San Pedro s/n, Torre sur, 4a planta, Universidad de Cádiz, 11510, Puerto Real, Cádiz, Spain
[b] Department of Chemistry, University of Sussex, Brighton, Sussex, BN1 9QJ, United Kingdom
[c] Faculdade de Ciências Farmacêuticas de Ribeirão Preto, Universidade de São Paulo, 14040-903 Ribeirão Preto, Brazil

ARTICLE INFO

*Keywords:*
*Botrytis cinerea*
Sclerotiniaceae
Biosynthesis
Cryptic metabolites
Eremophilenols

ABSTRACT

A thorough study of the fermentation broth of three strains of *Botrytis cinerea* which were grown on a modified Czapek-Dox medium supplemented with 5 ppm copper sulphate, yielded five undescribed metabolites. These metabolites possessed a sesquiterpenoid (+)-4-*epi*-eremophil-9-ene carbon skeleton which was enantiomeric to that of the phytoalexin, capsidiol. The isolation of these metabolites when the fungus was stressed, suggests that they may be potential effectors used by *B. cinerea* to circumvent plant chemical defences against phytopathogenic fungi. The biosynthesis of these compounds has been studied using $^{2}H$ and $^{13}C$ labelled acetate.

## 1. Introduction

The ascomycete *Botrytis cinerea* Pers. Fr, classified within the family Sclerotiniaceae, is the causative agent of a grey mould disease which infects at least 1400 plant species (Elad et al., 2016), including crops of economic importance such as grapes and strawberries (Dean et al., 2012). The fungus is a typical necrotroph whose infective cycle includes the induction of plant cell death followed by the maceration of the plant tissue and then reproduction by forming asexual spores on the decomposing plant material. The emergence of the disease symptoms depends on the host plant, the infected part of the plant and the weather conditions (van Kan, 2006; Williamson et al., 2007). It has recently been reported that *B. cinerea* can also systemically colonize plants without causing disease symptoms (van Kan et al., 2014). In general, *B. cinerea* is responsible for severe economic losses that are either due to the damage to the growing plants in the field or to the subsequent decay of the harvested fruits, flowers and vegetables during storage under cold and humid conditions (van Kan, 2006; Williamson et al., 2007).

The wide host range of *B. cinerea* in contrast to other *Botrytis* species that are specialized on a single host species, e.g. *B. elliptica* on lilies, may be due to the formation of phytotoxic metabolites and proteins with necrotizing activities that are effective against a range of plant species. Thus *B. cinerea* produces specific terpenoid and polyketide metabolites such as the sesquiterpene botrydial (**1**) and related compounds (Colmenares et al., 2002), botrylactone (**2**) and the botcinic (**3**) and botcineric acids (**4**) as well as their cyclic relatives, the botcinins (**5**, **6**) (Tani et al., 2005, 2006). The sesquiterpenoid abscisic acid (**7**) (Marumo et al., 1982) which mediates leaf fall and the polyketide, cinbotolide (**8**) have also been isolated from the fungus (Fig. 1) (Botubol et al., 2014; Collado and Viaud, 2016).

It is now clear that the development of pathogenesis by *B. cinerea* is much more complex than previously believed. Disease progression is tightly regulated throughout the infection process and the fungus undergoes developmental adaptions that coincide with the different stages of the infection. The interactions between the fungus and the plant are mediated by compounds which affect both the fungus and the plant (González et al., 2016). One class of such compounds are the effectors. These compounds are secreted by a microbial pathogen in order to inhibit the plant defensive system (Maffei et al., 2012). In many plant-pathogen interactions, effectors are key pathogenicity determinants that modulate the plant's intrinsic immunity to facilitate the development of the parasitic infection (Oliva et al., 2010). Thus the discovery of the fungal effectors produced by *B. cinerea* and the identification of

* Corresponding author.
*E-mail address:* isidro.gonzalez@uca.es (I.G. Collado).

https://doi.org/10.1016/j.phytochem.2018.06.010
Received 9 March 2018; Received in revised form 11 June 2018; Accepted 12 June 2018

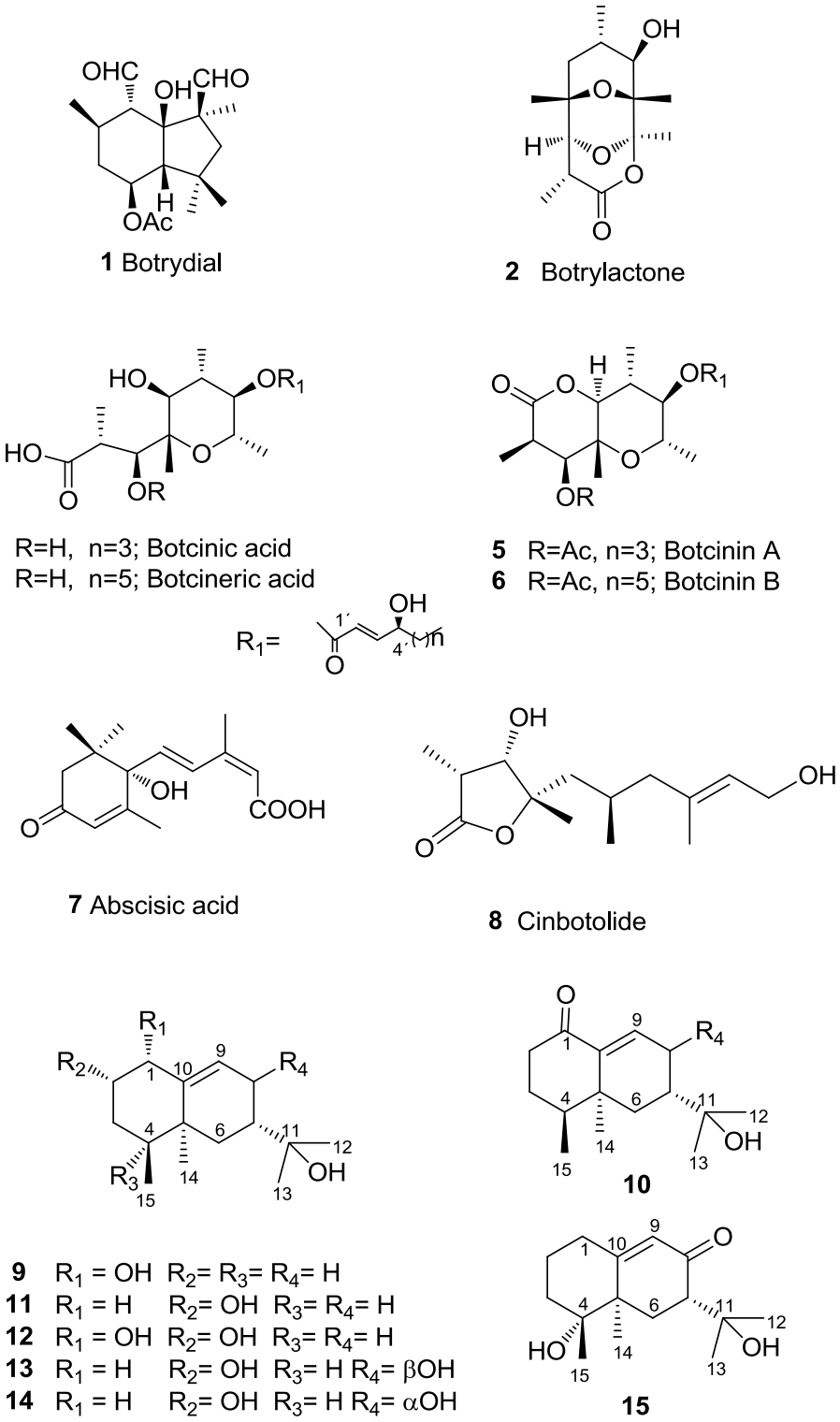


**Fig. 1.** Some metabolites isolated from *B. cinerea*.

their plant targets holds promise for the improvement of plant tolerance to this serious pathogen.

The recent sequencing of the *B. cinerea* genome has provided an opportunity to discover novel biosynthetic gene clusters involved in the biosynthesis of novel fungal metabolites. Forty-four genes that encode key enzymes have been identified including those involved in the biosynthesis of terpenes, polyketides and peptides that are specific to this phytopathogen (Amselem et al., 2011). The genome has shown that the biosynthetic potential of this microorganism has been barely explored and, as a result, a significant number of metabolites remain to be discovered. Consequently *B. cinerea* is a valuable organism with which to study the role of orphan biosynthetic genes and cryptic metabolites (Scherlach and Hertweck, 2009). In this context we have recently described the induction of a silent eremophilene biosynthetic pathway using sub-lethal doses of copper ions and characterized an undescribed family of eremophilenols (**9**–**15**) as cryptic metabolites (Pinedo et al., 2016).

These metabolites, which have sporogenic activity, possess a (+)-5-

*epi*-aristolochene or (+)-4-*epi*-eremophil-9-ene carbon skeleton and are enantiomeric to the phytoalexin capsidiol and its derivatives (Pinedo et al., 2016). This paper deals with the isolation and elucidation of the structure of five cryptic eremophilenols from *B. cinerea* and the biosynthetic pathway leading to their formation from $^{13}C$ and $^{2}H$-labelled acetates.

## 2. Results and discussion

A mixture of the major cryptic metabolites (**11–13**) from the group of eremophilenols (**9–15**) which we had isolated previously, was submitted to conidiation-inducing experiments (Pinedo et al., 2016). The increase in the formation of conidiophores was 5–6 times greater with the strain *B. cinerea* B05.10 and three fold greater with *B. cinerea* UCA 992 when compared to controls (Pinedo et al., 2016). This led us to conclude that the reported eremophilenols were involved in conidiation and in the self-regulation of the production of asexual spores (Pinedo et al., 2016). Consequently we have carried out a more detailed study of the chemical induction of the silent eremophilene biosynthetic pathway.

The strains *B. cinerea* UCA992, B05.10 and the double-mutant from the B05.10 strain, *BcBOT2ΔBcBOA6Δ*, were grown on a modified Czapek-Dox medium containing 5 ppm copper sulphate. The broths from the different fermentations were extracted with EtOAc and the extracts separated by column chromatography. The fractions containing eremophilene derivatives were submitted to HPLC chromatography to obtain pure compounds, which were characterized by extensive NMR experiments. In addition to the known compounds indicated in the experimental section (Pinedo et al., 2016), the following products were isolated: compounds **16–18** were obtained from *B. cinerea* UCA992, **16** and **19** from B05.10 and compound **20** was obtained from *BcBOT2ΔBcBOA6Δ* (Fig. 2).

The molecular formula for compound **16** was established as $C_{15}H_{26}O_2$ by HRMS. This was consistent with the $^{13}C$ NMR and HSQC data and implied three degrees of unsaturation. The $^{13}C$ NMR revealed the presence of four methyl, five methylene, two methine groups and four quaternary carbons, two of which bore an oxygen function. The $^{1}H$ NMR spectrum contained a signal at $\delta$ 5.49 which was characteristic of one proton on a trisubstituted double bond, together with four three-proton singlet signals at $\delta$ 1.23, 1.20, 1.19 and 1.13. The $^{1}H$ and $^{13}C$ NMR spectra were very similar to those reported previously for (+)-4α,11-dihydroxy-4-*epi*-eremophil-9-en-8-one (**15**) except for the absence of the C-8 carbonyl signal. In its place there were $^{1}H$ and $^{13}C$ NMR signals at $\delta$ 2.05 and 25.7 in accord with structure **16**.

The stereochemistry of the asymmetric carbons was confirmed by

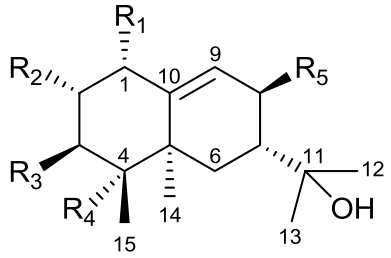


**16** $R_1 = R_2 = R_3 = R_5 = H$; $R_4 = OH$
**17** $R_1 = R_2 = R_3 = R_4 = H$; $R_5 = OH$
**18** $R_1 = R_2 = R_3 = H$; $R_4 = R_5 = OH$
**19** $R_1 = R_3 = R_4 = H$; $R_2 = OH$; $R_5 = O$
**20** $R_1 = R_3 = OH$; $R_2 = R_4 = R_5 = H$
**20a** $R_1 = R_3 = OAc$; $R_2 = R_4 = R_5 = H$

**Fig. 2.** (+)-4-*epi*-eremophilene derivatives isolated from *B. cinerea* strains.

the nOe interactions (see Table S1 in the supplementary data). Irradiation of H-15β produced nOe enhancements of the signals corresponding to H-1β, H-2, H-3β, H-6β, and H−7β whilst irradiation at H-14α produced a nOe effect at H-3α and H-6α. Analysis of the $^{1}H$-$^{1}H$ COSY, NOE and $^{1}H$-$^{13}C$ heteronuclear correlation spectra (HSQC and HMBC) led to the assignment of all the proton and carbon signals confirming the relative stereochemistry and structure of compound **16** as (4R,5R, 7*S*)-eremophil-9-ene-4,11-diol.

The $^{1}H$ and $^{13}C$ NMR spectra of compound **17**, $C_{15}H_{26}O_2$, had a pattern of signals that were characteristic of an eremophilene. There were $^{13}C$ NMR signals at $\delta$ 75.2 (s, C-11), 30.1 (q, C-12) and 23.7 (q, C-13), which were assigned to a *gem*-dimethyl group attached to a hydroxylated carbon at C-11. In the HMBC spectrum there were correlations between H-12 and H-13 and the signals corresponding to the carbons C-7, C-11, C-12/C-13. There was a $^{1}H$ NMR signal at $\delta$ 4.25 (1H, ddd, $J$ = 9.3, 3.3 and 1.4 Hz). This was assigned to a secondary alcohol which was located at C-8 because in the two-dimensional spectrum there were HMBC correlations between this resonance and C-9 and C-10 and between H-6 and C-7 and C-8. The stereochemistry at C-4, C-7 and C-8 followed from the magnitudes of the $^{1}H$-$^{1}H$ coupling constants. Thus H-4 ($\delta$ 1.6), with α disposition, was a quartet of double-doublets, ($J$ = 7.1, 4.8 and 2.2 Hz) and H-7 (β) ($\delta$ 1.78) was doublet of double-doublets, ($J$ = 13.8, 9.3 and 3.5 Hz). The signal assigned to H-8 showed a coupling to H-7 ($J$ = 9.3 Hz) and to H-9 ($J$ = 1.4 Hz). Molecular models reveal the possibility of a hydrogen bond involving the hydroxyl groups at C-8 and C-11. The consequent reduction in the rate of exchange of the hydroxyl hydrogen, which appear superimposed at $\delta$ 2.25, as deduced from the observed correlation in the COSY experiment, leads to the additional coupling of H-8 as 3.3 Hz. Furthermore the presence of this hydrogen bond restricts the rotation of the C-7/C-11 bond placing the methyl groups C-12 and C-13 in different environments. This is reflected in their $^{13}C$ NMR chemical shifts ($\delta$ 23.7 and 30.1) when compared to **16** ($\delta$ 27.0 and 27.2) where there is no hydrogen bond. The coupling constants of **17** were identical to those for the same signals in **13** whose absolute configuration had been determined by Mosher's method (Pinedo et al., 2016). A detailed analysis of the COSY, NOESY, HSQC and HMBC spectra (Table S2, supplementary data) led to the assignment of all the proton and carbon signals and confirmed the structure of **17** as (4*S*,5*S*,7R,8R)-eremophil-9-ene-8,11-diol.

Compound **18** had a molecular ion corresponding to $C_{15}H_{26}O_3$ and possessed signals in its $^{1}H$ NMR spectrum which resembled those of compound **17** except for the presence of four three-proton singlets in place of the three singlets and one doublet observed in **17**. This suggested that compound **18** had a structure corresponding to **17** with an additional hydroxyl group geminal to the methyl group at C-4. This structure was confirmed by the COSY, HSQC and HMBC experiments (Table S3). The couplings observed in the HSQC and COSY spectra led to the assignment of all fifteen signals in the $^{13}C$ NMR spectrum. The HMBC correlations between H-6 and C-4, C-5, C-7, C-8, C-11 and C-14 and between H-12/H-13 and C-7, C-11, C-12/C-13 located the two tertiary hydroxyl groups at C-4 and C-11 and the secondary hydroxyl group at C-8. The stereochemistry of the hydroxyl groups at C-4 and C-8 followed from nOe studies and the coupling constants for H-8. Thus irradiation of the methyl group H-15β produced nOe enhancements at H-6β and H-7 consistent with the α-orientation of the hydroxyl group at C-4 whilst irradiation of the signal for H-8 led to the enhancement of H-12/H-13. The coupling pattern of the H-8 signal ($\delta$ 4.26, ddd, $J$ = 9.3, 3.4 and 1.5 Hz) was identical to that of compound **13** and compound **17**. The hydroxyl group at C-8 was therefore assigned the β-configuration with a hydrogen bond to the hydroxyl group at C-11 accounting for the additional coupling of 3.4 Hz. Consequently compound **18** had the structure (4R,5R,7R, 8R)-eremophil-9-ene-4,8,11-triol.

Compound **19** had a molecular ion corresponding to $C_{15}H_{24}O_3$. The $^{13}C$ NMR spectrum revealed the presence of four methyl, three methylene and four methine groups together with four quaternary

carbons, one of which at $\delta$ 203.0 ppm corresponded to a carbonyl group. The $^{1}$H NMR spectrum showed, in addition to the signals for four methyl groups at $\delta$ 1.12 (3H, d, $J$ = 7.3 Hz), 1.21 (6H, s) and 1.34 (3H, s), a pattern of signals that were characteristic of an eremophilene derivative with two hydroxyl groups. The spectra were very similar to those for compound **11** which possessed two hydroxyl groups at C-2 and C-11. The principal difference was the presence in the $^{13}$C NMR spectrum of the signal for the carbonyl group at $\delta$ 203.0 ppm and the deshielding in the $^{1}$H NMR spectrum of the signal for H-9 to $\delta$ 5.92. This indicated the presence of a $\Delta^{9,10}$ 8-keto-α,β-unsaturated ketone. The proposed structure **19** was supported by the correlations which were observed in the COSY, HSQC and HMBC spectra (Table S4). The stereochemistry was assigned by extensive nOe experiments. Irradiation of the proton geminal to the hydroxyl group at C-2 produced nOe enhancements of the signals corresponding to H-1β and H-15β. Irradiation of the signals for H-7β and H-15β produced nOe effects at H-12, H-13 and H-15β, and H-2β and H-7β, respectively. This data, together with the large number of correlations in the HMBC experiment (Table S4) were in accord with the structure and stereochemistry shown for compound **19** as (2*S*,4*S*,5*S*,7*S*)-2,11-dihydroxy-eremophil-9-en-8-one.

Compound **20** also showed a pattern of $^{1}$H and $^{13}$C NMR signals characteristic of an eremophilenol containing two secondary and one tertiary hydroxyl groups. A preliminary study of these spectra indicated a similarity to capsidiol (**21**) (Fig. 3) except for the absence of the signals corresponding to the protons and carbons of the isopropenyl group. Instead the $^{1}$H NMR spectrum contained two methyl group singlets at $\delta$ 1.18 and 1.20 and a signal in the $^{13}$C NMR spectrum at $\delta$ 72.7 characteristic of a 2-hydroxypropan-2-yl group at C-7. The molecular formula, $C_{15}H_{26}O_3$, deduced from the HRMS and the data obtained from the COSY, NOESY, HSQC and HMBC experiments were consistent with the structure **20** of an 11-hydroxy relative of capsidiol (**21**) (Table S5).

In order to correlate the compounds **20** and **21**, natural capsidiol (**21**) was isolated from green peppers treated with aq. cellulase following a modification to the procedures of Whiteheah et al. (1987) and Zhao et al. (2004) (see experimental section). Capsidiol (**21**) was acetylated with acetic anhydride in pyridine to give the known diacetate **21a** which possessed identical data to that reported in the literature (Zhao et al., 2004). This was then submitted to an oxymercuration-demercuration reaction (Blay et al., 2001) to give compound **22** in good yield. Compound **20** was also acetylated by the conventional method to yield the diacetate **20a** (Table S6). Both compounds had identical spectroscopic data but their optical rotations were of opposite sign, **20a** $[\alpha]_D^{21}$-20°, **22** $[\alpha]_D^{21}$ +27.5°. This data confirmed that the phytopathogenic fungus *B. cinerea* has afforded a family of eremophilenes (**16**–**20**) with skeleton that are enantiomeric to those of the phytoalexin, capsidiol (**21**) and its relatives.

We have shown that the induction of conidiation and spore formation in *B. cinerea* as a result of the stress of sub-lethal concentrations of copper ions is mediated by the formation of eremophilenols by the fungus (Pinedo et al., 2016). Their enantiomeric relationship to the phytoalexin capsidiol, raises the interesting possibility that they may also be involved in the fungal response to the antifungal activity of the phytoalexin by, for example, regulating the biosynthesis of the phytoalexins in the host plant.

### 2.1. Biosynthesis of (+)-4-epi-eremophil-9-en-11-ols

Aristolochene is a sesquiterpenoid diene which occurs naturally in two enantiomeric forms. (−)-Aristolochene has been isolated from plants including the roots of *Aristolochia indica* (Govindachari et al., 1970) and from insect sources (Baker et al., 1981) whilst (+)-aristolochene is of fungal origin (*Aspergillus terreus*) (Cane et al., 1987). Previous biosynthetic studies have established that (+)-aristolochene is formed by the cyclization of (*E*,*E*)-farnesyl diphosphate (FDP) via the intermediate (*S*)-(−)-germacrene A as the U,U-conformer (C-14 and C-15 methyls Up) (Faraldos et al., 2010). The protonation of the germacrene A leads to cyclization and the formation of the bicyclic *trans*-fused eudesmane cation. Successive 1,2-hydride and methyl group rearrangements followed by the loss of the pro-*S* hydrogen from C-9 generates (+)-aristolochene (Fig. 4, route a) (Faraldos et al., 2010). (*R*)-Germacrene A exists as three NMR-distinguishable conformers UU (Up C10-Me, Up C4-Me), UD (Up C10-Me, Down C4-Me) and DU (Down C10-Me, Up C4-Me), (Fig. 4), in a ratio of 5:3:2 at or below 25 °C (Faraldos et al., 2007). Under similar conditions the related sesquiterpene alcohol, hedycaryol (Fig. 4) exists in soln. in the same three forms, except that the UD and DU conformers predominate over the UU alternative due to the larger steric bulk of the hydroxypropyl substituent (Ōsawa et al., 1979; Terada and Yamamura, 1979; Wharton et al., 1973). Hence it is plausible that, through the action of a hitherto unidentified enzyme, (*E*,*E*)-FDP is transformed to (*S*)-hedycaryol whose DU conformer would lead via an acid-catalysed cyclization to an *epi*-eudesmyl cation with the correct stereochemistry to act as a precursor to the (+)-5-*epi*-aristoloch-9-en-11-ols, also known as (+)-4-*epi*-eremophil-9-en-11-ols (Fig. 4, route b). In order to explore this hypothesis, biosynthetic experiments with sodium [1–$^{13}$C]-, [2–$^{13}$C]- and [$^{2}H_3$]-acetates have been carried out with resting cell cultures of the *B. cinerea* mutant *BcBOT2Δ*.

The optimum times for feeding the precursors to resting cell cultures of *BcBOT2Δ* have been established as result of the time-course study for the production of (+)-4-*epi*-eremophil-9-en-2α,11-diol (**11**). Consequently 5 days old resting cell cultures of this mutant were fed with the labelled sodium acetates and the resultant (+)-4-*epi*-eremophil-9-en-2α,11-diols (**11**) were extracted, purified and analyzed by $^{13}$C and $^{2}$H NMR spectroscopy (Table 1).

Significant enrichments were observed for C-2, C-4, C-6, C-8, C-10 and C-11 from the sodium [1–$^{13}$C]-acetate whilst the sodium [2–$^{13}$C]-acetate led to enhanced signals for C-1, C-3, C-7, C-9, C-12, C-13 and C-15. Furthermore the enhanced signals for C-5 and C-14 showed characteristic satellite signals arising by $^{13}$C-$^{13}$C spin-spin coupling

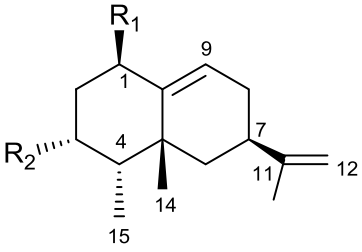


**21** $R_1 = R_2 = OH$
**21a** $R_1 = R_2 = OAc$

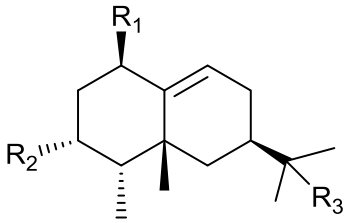


**22** $R_1 = R_2 = OAc$, $R_3 = OH$

**Fig. 3.** Capsidiol (**21**) and derivatives.

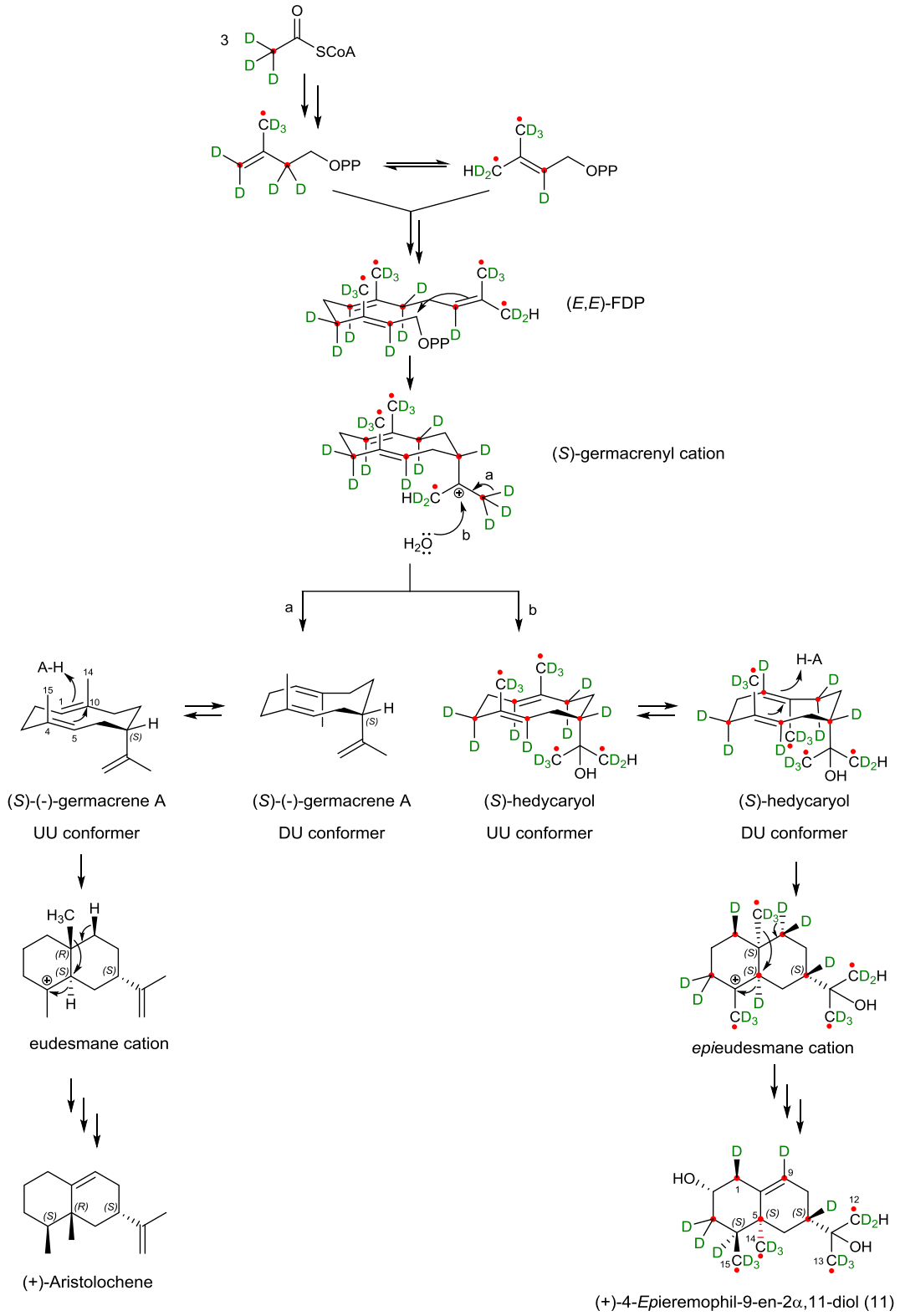


**Fig. 4.** Proposed biosynthetic route to (+)-4-*epi*-eremophilenols. Labelling pattern resulting from feeding experiments with sodium [2–$^{13}$C]- and [$^{2}H_3$]-acetates.

(Table 1). This coupling indicated that a 1,2-methyl migration had occurred suggesting that the biosynthesis of the compound **11** from (*E*,*E*)-FDP had followed the folding outlined in Fig. 4 (route b).

A further feeding experiment with sodium [$^{2}H_3$]-acetate gave additional evidence to support this hypothesis. The incorporation of the labelled precursor into **11** was analyzed by $^{2}$H NMR. Although there was only a low incorporation, the signals corresponding to D-1β, D-3, D-4, D-7, D-9 and to the methyl groups D-12, D-13, D-14 and D-15 were unambiguously identified. The presence of a deuterium atom at C-4 corresponded to a 1,2-hydride migration from C-5 to C-4 of the eudesmane cation during the biosynthesis (Fig. 4).

These data are consistent with the biosynthetic pathway outlined in Fig. 4 (route b) in which the (+)-4-*epi*-eremophil-9-en-11-ols are biosynthesised by cyclization of (*E*,*E*)-FDP via (*S*)-hedycaryol. Protonation

**Table 1**
Isotopic enrichment of carbons and coupling constants in (+)-4-*epi*-eremophil-9-en-2α,11-diol (**11**) after feeding sodium [1–$^{13}$C]- and [2–$^{13}$C]-acetates to *BcBOT2Δ*.

| Carbon atom (*N*) | $\delta_C$ ($CDCl_3$) | Atom % $^{13}$C excess [a] | | $^1J_{CC}$ (Hz) |
|---|---|---|---|---|
| | | [1–$^{13}$C]-acetate | [2–$^{13}$C]-acetate | |
| 1 | 41.64 | 0.15 | 6.95 | |
| 2 | 67.69 | 3,63 | −0.19 | |
| 3 | 39.685 | 0.27 | 8.30 | |
| 4 | 41.38 | 3.12 | −0.20 | |
| 5 | 37.925 | 0.59 | 4.00 | 38 |
| 6 | 38.39 | 3.16 | 0 | |
| 7 | 42.98 | −0.02 | 7.91 | |
| 8 | 25.96 | 3.52 | −0.20 | |
| 9 | 123.38 | −0.06 | 9.28 | |
| 10 | 137.89 | 1.95 | −0.55 | |
| 11 | 72.62 | 2.38 | −0.68 | |
| 12 | 27.12[b] | 0.03 | 7.43 | |
| 13 | 27.08[b] | 0.17 | 10.06 | |
| 14 | 30.26 | 0.18 | 4.26 | 38 |
| 15 | 18.60 | 0 | 7.78 | |

[a] Atom % $^{13}$C excess = {($R_N$/$R_{N(UL)}$ x 1.1} – 1.1, where $R_N$ is the ratio of the peak intensity at *N*-position in labelled compound calculated on the basis of the peak intensity at the C-15-position in [1–$^{13}$C]-acetate and C-6-position in [2–$^{13}$C]-acetate. Similarly, $R_{N(UL)}$ is the ratio of the peak intensity at *N*-position in unlabeled compound. Value 1.1 is the theoretical $^{13}$C natural abundance (atom %).

[b] Interchangeable signals.

at C-1 of the DU conformer of (*S*)-hedycaryol and attack by the C-4/C-5 (pi) bond on the resulting C-10 carbocation leads to the *cis*-fused eudesmane cation. This generates the (+)-4-*epi*-eremophil-9-en-11-ols after successive 1,2-hydride and methyl group migrations followed by the loss of the pro-*R* hydrogen from C-9.

## 3. Conclusions

Five undescribed eremophilenol derivatives **16–20** have been isolated from 27 days old cultures of the strains of *B. cinerea* UCA992, B05.10 and the double mutant from the B05.10 strain, *BcBOT2ΔBcBOA6Δ*. Their structures have been established and, interestingly, these compounds have been shown to possess an underlying carbon skeleton which is enantiomeric to that of the phytoalexin capsidiol (**21**), which is produced by green peppers when they are infected by phytopathogenic fungi. Indeed the metabolite of *B. cinerea*, compound **20**, is *ent*-11-hydroxydihydrocapsidiol. This suggests that the eremophilenols of *B. cinerea* may also be effectors inhibiting the plant defences or modulating the plant immunity in order to facilitate the progress of the infection. Finally, using labelled acetates, a biosynthetic pathway has been established involving the probable transformation of (*E*,*E*)-FDP via (*S*)-hedycaryol and cyclization of its DU conformer to a *cis*-fused eudesmane cation and thence the (+)-4-*epi*-eremophilenol derivatives.

## 4. Experimental

### 4.1. General experimental procedures

TLC was performed on Merck Kiesegel 60 $F_{254}$, 0.25 mm thick. Silica gel 60$PF_{254}$ (60–100 mesh, Merck) was used for column chromatography. HPLC was performed with a Hitachi/Merck L-6270 apparatus equipped with an UV-VIS detector (L 4250) and a differential refractometer detector (RI-7490). Lichrosfer Si 60 (5 μm) LichoCart (250 mm × 4 mm) and Lichrosfer Si 60 (10 μm) LichoCart (250 mm × 10 mm) columns were used for isolation experiments. Infrared spectra were recorded on a FT-IR spectrophotometer, Perkin Elmer, Spectrum BX FTIR System, and reported as wave number ($cm^{-1}$). $^1$H and $^{13}$C NMR measurements were recorded on Agilent 500 and 600 MHz spectrometers with $SiMe_4$ as the internal reference. Chemical shifts were referenced to $CDCl_3$ ($\delta_H$ 7.25, $\delta_C$ 77.0). NMR assignments were made using a combination of 1D and 2D techniques. High-Resolution Mass Spectroscopy (HRMS) was performed in a QTOF mass spectrometer, (Water, Synapt G2), in positive or negative ion ESI or APCI modes.

### 4.2. Labelled precursors

Sodium [1–$^{13}$C]- (99%), [2–$^{13}$C]- (99%), and [$^2H_3$]-acetates (99%) were obtained from Cambridge Isotope Laboratories, Inc. (Andover, MA, USA). All samples were dissolved in water and sterilized through 0.22 μm Millex GP (Millipore) filters before being added to the fermentation flasks.

### 4.3. Microorganisms

4 The genus *Botrytis* Pers. is classified within the family Sclerotiniaceae Whetz. Four strains were used in this work: wild types *B. cinerea* UCA 992 and B05.10, and the mutants *BcBOT2ΔBcBOA6Δ* and *BcBOT2Δ*. *B. cinerea* UCA 992 was obtained from grapes from the Domecq vineyard, Jerez de la Frontera, Cádiz, Spain. This culture is deposited in the University of Cádiz, Mycological Herbarium Collection (UCA). Strain B05.10 of *B. cinerea* Pers. Fr. was isolated from a *Vitis* field sample (Quidde et al., 1998). The double mutant *BcBOT2ΔBcBOA6Δ* (Dalmais et al., 2011), and the mutant *BcBOT2Δ* (Pinedo et al., 2008) were supplied by Dr. Muriel Viaud, and are maintained in the UMR BIOGER strain collection, INRA (Grignon, France). Conidial stock suspensions of all of these strains were maintained viable in 80% glycerol at −40 °C.

### 4.4. Culture conditions and isolation of eremophilenols

5 B. *cinerea* strains were grown at 25 °C in Roux culture bottles (200 ml), each containing 150 ml of modified Czapek-Dox medium (50.0 g glucose, 1.0 g yeast extract, 5.0 g $K_2HPO_4$, 2.0 g $NaNO_3$, 0.5 g $MgSO_4$ $7H_2O$, 0.01 g $FeSO_4$ $7H_2O$, 0.005 g $CuSO_4{\cdot}5H_2O$, pH 7, 1 L of water) (Pinedo et al., 2016). Each bottle was inoculated with 1,1 × $10^6$ fresh conidia obtained from a 18 days old culture of *B. cinerea* on Agar-Malt medium, and then incubated for 27 days at 24–26 °C on surface cultures under white light (day light lamp) for metabolite production.

The broths (3l) from each of the strains (*B. cinerea* UCA992, B05.10 and *BcBOT2ΔBcBOA6Δ*), were filtered, satd. with NaCl and extracted with EtOAc (x4). The organic extracts were washed with $H_2O$ (x3) and then dried over dry $Na_2SO_4$. Evaporation of the solvent at reduced pressure gave the extracts as yellow oils, 180 mg (from *B. cinerea* UCA 992), 140 mg (B05.10) and 160 mg (*BcBOT2ΔBcBOA6*).

A preliminary fractionation of the extracts was achieved by column chromatography on silica gel eluting with *n*-hexane-EtOAc mixtures containing increasing percentages of EtOAc (9:1 → 0:1). Final purification of the fractions of interest were carried out by means of semipreparative HPLC using *n*-hexane-EtOAc-acetone (7:2:1) as the mobile phase and flow rate 2.5 ml/min.

The broth of *B. cinerea* UCA992 gave, in addition to the known compounds **9** (1.0 mg), **11** (1.1 mg), **12** (3.2 mg), and **13** (2.0 mg), the metabolites **16** (1.1 mg), **17** (1.2 mg), and **18** (0.7 mg). Strain B05.10 broth afforded the known compounds **11** (3.1 mg), **12** (2.8 mg), and **13** (3.0 mg), and the specialized metabolites **16** (0.7 mg), and **19** (1.0 mg). The mutant *BcBOT2ΔBcBOA6* yielded, in addition to the metabolites **11–15** (1.0, 0.8, 1.5, 1.3, 1.1 mg, respectively), an undescribed metabolite **20** (0.8 mg).

#### 4.4.1. (4R, 5R, 7S)-eremophil-9-ene-4,11-diol (16)

Colourless oil, $[\alpha]_D^{21}$ -3.7° (0.07c, $CHCl_3$). IR $\nu_{max}$ ($cm^{-1}$): 3420,

2932, 1372, 1103, 925.$^1$H NMR (600 MHz, $CDCl_3$): $\delta$ 0.91 (t, 1H, $J$ = 13.8 Hz, H-6α), 1.13 (s, 3H, H-14), 1.19 (s, 3H, H-12*), 1.20 (s, 3H, H-13*), 1.23 (s, 3H, H-15), 1.34 (m, 1H, H-1β), 1.34 (m, 1H, H-2β), 1.50 (m, 1H, H-3β), 1.69 (m, 1H, H-7β), 1.69 (m, 1H, H-2α), 1.87 (td, 1H, $J$ = 13.6, 4.6 Hz, H-3α), 1.96 (m, 1H, H-1α), 2.05 (m, 2H, H-8), 2.24 (dt, $J$ = 13.8, 2.5 Hz, H-6β), 5.49 (dt, 1H, $J$ = 6.7, 1.7 Hz, H-9). $^{13}$C NMR (150 MHz, $CDCl_3$): $\delta$ 24.3 ($CH_2$, C-2), 25.4 ($CH_3$, C-14), 25.7 ($CH_2$, C-8), 25.9 ($CH_3$, C-15), 27.0 ($CH_3$, C-12*), 27.2 ($CH_3$, C-13*), 31.0 ($CH_2$, C-1), 33.4 ($CH_2$, C-6), 38.5 ($CH_2$, C-3), 43.3 (CH, C-7), 43.6 (C, C-5), 72.7 (C, C-11), 75.6 (C, C-4), 121.0 (CH, C-9), 142.0 (C, C-10), *interchangeable assignments. HRMS(ESI$^+$): calcd. for $C_{15}H_{26}O_2Na$ [M + Na]$^+$ 261.1830, found 261.1831; calcd. for $C_{15}H_{25}O$ [M + H-$H_2O$]$^+$ 221.1905, found 221.1901; calcd. for $C_{15}H_{23}$ [M + H-2$H_2O$]$^+$ 203.1800, found 203.1800; calcd. for $C_{12}H_{17}$ [M + H-$H_2O$-$(CH_3)_2CO$]$^+$ 161.1330, found 161.1330.

#### 4.4.2. (4S, 5S, 7R, 8R)-eremophil-9-ene-8,11-diol (17)

Colourless oil, $[\alpha]_D^{21}$ +8.2° (0.13 c, $CHCl_3$). IR $\nu_{max}$ (cm$^{-1}$): 3331, 2932, 1464, 1377, 1172, 1034.$^1$H NMR (500 MHz, $CDCl_3$): $\delta$ 1.00 (d, 3H, $J$ = 7.1 Hz, H-15), 1.05 (t, 1H, $J$ = 14 Hz, H-6) 1.14 (s, 3H, H-14), 1.21 (s, 3H, H-13*), 1.31 (s, 3H, H-12*), 1.30 (m, 1H, H-3′), 1.50 (m, 2H, H-2, H-2′), 1.50 (dd, 1H, $J$ = 14, 3.5 Hz, H-6′), 1.60 (qdd, 1H, $J$ = 7.1, 4.8, 2.2 Hz, H-4α), 1.78 (ddd, 1H, $J$ = 13.8, 9.3, 3.5 Hz, H-7β), 1.98 (m, 1H, H-3), 2.00 (m, 1H, H-1′), 2.25 (m, 1H, H-1), 2.22–2.26 (m, 1H(superimposed), C8-OH), 4.25 (ddd, 1H, $J$ = 9.3, 3.3, 1.4 Hz, H-8α), 5.40 (t, 1H, $J$ = 1.8 Hz, H-9). $^{13}$C NMR (125 MHz, $CDCl_3$): $\delta$ 17.6 ($CH_3$, C-15), 21.8 ($CH_2$, C-2), 23.7 ($CH_3$, C-13*), 30.0 ($CH_2$, C-3), 30.1 ($CH_3$, C-12*), 30.4 ($CH_3$, C-14), 31.4 ($CH_2$, C-1), 38.3 ($CH_2$, C-6), 38.8 (C, C-5), 41.2 (CH, C-4), 49.3 (CH, C-7), 69.7 (CH, C-8), 75.2 (C, C-11), 126.0 (CH, C-9), 141.8 (C, C-10), *interchangeable assignments. HRMS(ESI$^+$): calcd. for $C_{15}H_{27}O_2$ [M + H]$^+$ 239.2011, found 239.1992.

#### 4.4.3. (4R, 5R, 7R, 8R)-eremophil-9-ene-4,8,11-triol (18)

Colourless oil, $[\alpha]_D^{21}$-3.8° (0.15c, $CHCl_3$). IR $\nu_{max}$ (cm$^{-1}$): 3363, 2933, 1674, 1464, 1368, 1067.5, 924.5.$^1$H NMR (500 MHz, $CDCl_3$): $\delta$ 0.80 (t, 1H, $J$ = 14.5 Hz, H-6α), 1.11 (s, 3H, H-14), 1.23 (s, 3H, H-12*), 1.30 (s, 3H, H-15), 1.35 (s, 3H, H-13*), 1.42 (m, 1H, H-2′), 1.51 (m, 1H, H-3β), 1.72 (m, 1H, H-2), 1.80 (dd, 1H, $J$ = 9.3, 3.5 Hz, H-7β), 1.84 (m, 1H, H-3α), 2.04 (m, 1H, H-1β), 2.10 (dd, 1H, $J$ = 14.5, 3.5 Hz, H-6β), 2.26 (m, 1H, H-1α), 4.26 (ddd, 1H, $J$ = 9.3, 3.4, 1.5 Hz, H-8), 5.38 (t, 1H, $J$ = 1.8 Hz, H-9). $^{13}$C NMR (125 MHz, $CDCl_3$): $\delta$ 23.6 ($CH_3$, C-12*), 24.0 ($CH_2$, C-2), 25.6 ($CH_3$, C-14), 25.7 ($CH_3$, C-15), 30.3 ($CH_3$, C-13*), 30.4 ($CH_2$, C-1), 32.4 ($CH_2$, C-6), 38.5 ($CH_2$, C-3), 43.5 (C, C-5), 49.3 (CH, C-7), 69.3 (CH, C-8), 75.5 (C, C-11), 75.5 (C, C-4), 126.4 (CH, C-9), 142.5 (C, C-10), *interchangeable assignments. HRMS(ESI$^+$): calcd. for $C_{15}H_{26}O_3Na$ [M + Na]$^+$ 277.1780, found 277.1778; calcd. for $C_{15}H_{23}O$ [M + H-2$H_2O$]$^+$ 219.1749, found 219.1749; calcd. for $C_{15}H_{21}$ [M + H-3$H_2O$]$^+$ 201.1643, found 201.1642; calcd. for $C_{12}H_{15}$ [M + H-2$H_2O$-$(CH_3)_2CO$]$^+$ 159.1174, found 159.1173.

#### 4.4.4. (2S, 4S, 5S, 7S)-2,11-dihydroxyeremophil-9-en-8-one (19)

Colourless oil, $[\alpha]_D^{21}$ +9.9° (0.04c, $CHCl_3$). IR $\nu_{max}$ (cm$^{-1}$): 3369, 2924, 2853, 1741, 1652, 1464, 772.$^1$H NMR (400 MHz, $CDCl_3$): $\delta$ 1.12 (d, 3H, $J$ = 7.3 Hz, H-15), 1.21 (s, 3H, H-13*), 1.21 (s, 3H, H-12*), 1.34 (s, 3H, H-14), 1.62 (t, 1H, $J$ = 14.7 Hz, H-6β), 1.74 (dd, 1H, $J$ = 12.2, 4.4 Hz, H-3α), 2.00 (m, 1H, H-1α), 2.01 (m, 1H, H-3β), 2.03 (m, 1H, H-4α), 2.03 (m, 1H, H-6α), 2.52 (d, 1H, $J$ = 8.8 Hz, H-1β), 2.63 (dd, 1H, $J$ = 14.7, 6.2 Hz, H-7β), 3.90 (m, 1H, H-2β), 5.92 (s, 1H, H-9). $^{13}$C NMR (100 MHz, $CDCl_3$): $\delta$ 18.3 ($CH_3$, C-15), 24.1 ($CH_3$, C-12*), 28.1 ($CH_3$, C-13*), 31.1 ($CH_3$, C-14), 36.7 ($CH_2$, C-6), 39.3 (C, C-5), 39.4 ($CH_2$, C-3), 42.1 ($CH_2$, C-1), 42.1 (CH, C-4), 52.6 (CH, C-7), 67.9 (CH, C-2), 72.6 (C, C-11), 127.4 (CH, C-9), 164.3 (C, C-10), 203.0 (C, C-8), *interchangeable assignments. HRMS(ESI$^+$): calcd. for $C_{15}H_{25}O_3$ [M + H]$^+$ 253.1804, found 253.1807; calcd. for $C_{15}H_{23}O_2$ [M + H-$H_2O$]$^+$ 235.1698, found 235.1699; calcd. for $C_{15}H_{21}O$ [M + H-2$H_2O$]$^+$ 217.1592, found 217.1595.

#### 4.4.5. (1S, 3S, 4R, 5S, 7S)-eremophil-9-ene-1,3,11-triol (20)

Colourless oil, $[\alpha]_D^{21}$-6° (0.07c, $CHCl_3$). IR $\nu_{max}$ (cm$^{-1}$): 3463, 2972, 2934, 1370, 772.$^1$H NMR (500 MHz, $CDCl_3$): $\delta$ 0.85 (d, 3H, $J$ = 7.0 Hz, H-15), 1.18 (s, 3H, H-13*), 1.20 (s, 3H, H-12*), 1.22 (t, 1H, $J$ = 13.7 Hz, H-6), 1.36 (s, 3H, H-14), 1.62 (m, 1H, H-7β), 1.63 (m, 1H, H-2), 1.72 (m, 1H, H-8), 1.74 (m, 1H, H-4α), 1.80 (dt, 1H, $J$ = 13.7, 3.1 Hz, H-6′), 1.92 (m, 1H, H2′), 2.14 (ddt, 1H, $J$ = 16.0, 7.0, 3.5 Hz, H-8′), 4.34 (dd, 1H, $J$ = 3.8, 2.4 Hz, H-1β), 4.60 (dt, 1H, $J$ = 12.3, 4.6 Hz, H-3α), 5.91 (dd, 1H, $J$ = 7.0, 1.9 Hz, H-9). $^{13}$C NMR (125 MHz, $CDCl_3$): $\delta$ 9.1 ($CH_3$, C-15), 26.3 ($CH_2$, C-8), 27.0 ($CH_3$, C-12*), 27.3 ($CH_3$, C-13*), 32.3 ($CH_3$, C-14), 36.2 ($CH_2$, C-2), 38.9 (C, C-5), 40.7 ($CH_2$, C-6), 43.6 (CH, C-7), 47.8 (CH, C-4), 65.4 (CH, C-3), 72.4 (C, C-11), 74.9 (CH, C-1), 128.9 (CH, C-9), 140.4 (C, C-10), *interchangeable assignments. HRMS(ESI$^+$): calcd. for $C_{15}H_{23}O$ [M + H-2$H_2O$]$^+$ 219.1749, found 219.1751; calcd. for $C_{15}H_{21}$ [M + H-3$H_2O$]$^+$ 201.1643, found 201.1644; calcd. for $C_{12}H_{15}$ [M + H-2$H_2O$-$(CH_3)_2CO$]$^+$ 159.1174, found 159.1175.

### 4.5. Acetylation of (1S, 3S, 4R, 5S, 7S)-eremophil-9-en-1,3,11-triol (20)

Eremophilenetriol (**20**) (5.0 mg, 0.020 mmol) was dissolved in pyridine (0.5 ml) and stirred with acetic anhydride (1.0 ml, 0.011 mol) for 18 h. Then the reaction mixture was concentrated and purified by column chromatography to afford 5.0 mg of the diacetate derivative (**20a**).

#### 4.5.1. (1S, 3S, 4R, 5S, 7S)-1,3-diacetoxyeremophil-9-en-11-ol (20a)

Amorphous solid, $[\alpha]_D^{21}$-20° (0.05c, $CHCl_3$). $^1$H NMR (500 MHz, $CDCl_3$): $\delta$ 0.87 (d, 3H, $J$ = 7.1 Hz, H-15), 1.18 (s, 3H, H-13*), 1.19 (s, 3H, H-12*), 1.22 (t, 1H, $J$ = 13.6 Hz, H-6), 1.31 (s, 3H, H-14), 1.61 (m, 1H, H-7β), 1,73 (m, 1H, H-8′), 1.76 (m, 1H, H-6′), 1.79 (m, 1H, H-2'), 1.88 (m, 1H, H-2), 1.92 (m, 1H, H-4α), 2.02 (s, 3H, $CH_3CO$), 2.04 (s, 3H, $CH_3CO$), 2.15 (m, 1H, H-8), 5.39 (dd, 1H, $J$ = 4.0, 2.4 Hz, H-1β), 5.53 (dt, 1H, $J$ = 12.6, 4.6 Hz, H-3α), 6.08 (dd, 1H, $J$ = 7.1, 1.9 Hz, H-9).$^{13}$C NMR (125 MHz, $CDCl_3$) $\delta$ 170.3 (C, -OAc), 170.1 (C, -OAc), 135.3 (C, C-10), 132.0 (CH, C-9), 75.4 (CH, C-3), 72.3 (C, C-11), 69.3 (CH, C-3), 44.1 (CH, C-4), 43.2 (CH, C-7), 40.2 ($CH_2$, C-6), 38.9 (C, C-5), 31.0 ($CH_2$, C-2), 31.0 ($CH_3$, C-14), 27.1 ($CH_3$, C-12*), 27.0 ($CH_3$, C-13*), 26.3 ($CH_2$, C-8), 21.6 ($CH_3$, −$COCH_3$), 21.3 ($CH_3$, −$COCH_3$), 10.1 ($CH_3$, C-15), *interchangeable assignments. HRMS(ESI$^+$): calcd. for $C_{19}H_{30}O_5Na$ [M + Na]$^+$ 361.1991, found 361.1990; calcd. for $C_{15}H_{23}O$ [M + H-2AcOH]$^+$ 219.1749, found 219.1750; calcd. for $C_{15}H_{21}$ [M + H-2AcOH-$H_2O$]$^+$ 201.1643, found 201.1644; calcd. for $C_{12}H_{15}$ [M + H-2AcOH-$(CH_3)_2CO$]$^+$ 159.1174, found 159.1175.

### 4.6. Isolation of capsidiol (21) from green peppers

After removing the uppermost section of 23 green bell pepper fruits (*Capsicum annuum*) with a knife, the fruits were placed upright into trays and the exposed cavities filled with a 3 mg/l soln. of cellulase (*Trichoderma viride*) in deionized water. The fruits were incubated at 25 °C for 72 h after which time the aq. soln. was filtered through Nytal, pH adjusted to 6.7–7, and extracted with $CH_2Cl_2$ (2 × 0.25 ml/l of water soln.). Concentration of the combined $CH_2Cl_2$ layers and purification by column chromatography (*n*-hexane-EtOAc as eluents) provided 57.0 mg of pure capsidiol (**21**) (Whiteheah et al., 1987; Zhao et al., 2004).

### 4.7. Acetylation of capsidiol (21)

A soln. of capsidiol (**21**) (21.0 mg, 0.089 mmol) in pyridine (1 ml) and acetic anhydride (2.5 ml, 0.026 mol) was stirred for 18 h, then the reaction mixture was concentrated and purified by column chromatography affording 24.0 mg of the diacetate derivative **21a** (Zhao et al., 2004).

### 4.8. Preparation of (1R, 3R, 4S, 5R, 7R)-1,3-diacetoxyeremophil-9-en-11-ol (22) from capsidiol diacetate (21a)

Capsidiol diacetate (**21a**) (11.4 mg, 0.042 mmol) was dissolved in 0.5 ml of a THF-$H_2O$ mixture (1:1), and treated with $Hg(OAc)_2$ (17.5 mg, 0.055 mmol). The reaction mixture was stirred at rt for 30 min. To quench the reaction it was first diluted with ether (0.2 ml), cooled to 0 °C and it was treated drop wise with 3 M NaOH (0.1 ml) and 0.5 M $NaBH_4$ (0.1 mg) and 41.5 mg of NaCl. Then the reaction mixture was stirred at 0 °C for 10 min, diluted with ether and water and extracted in the usual way (Blay et al., 2001). The extract was purified by column chromatography, using *n*-hexane-EtOAc as eluent, yielding 7.0 mg of pure 1β,3α-diacetoxy derivative (**22**).

#### 4.8.1. (1R, 3R, 4S, 5R, 7R)-1,3-diacetoxyeremophil-9-en-11-ol (22)

Colourless oil, $[\alpha]_D^{21}$ +27.5° (0.43 c, $CHCl_3$). $^1$H NMR (500 MHz, $CDCl_3$): $\delta$ 0.86 (d, 3H, $J$ = 7.5 Hz, H-15), 1.16 (s, 3H, H-13), 1.17 (s, 3H, H-12), 1.22 (m, 1H, H-6β), 1.31 (s, 3H, H-14), 1.56 (m, 1H, H-7β), 1.71–1.80 (m, 3H, H-2α, H-8α, H-4α), 1.90 (m, 1H, H-6α), 2.01 (s, $CH_3$), 2.02 (m, 1H, H-2β), 2.03 (s, $CH_3$), 2.12 (m, 1H, H-8β), 5.38 (dd, 1H, $J$ = 2 Hz, H-1β), 5.53 (dt, 1H, $J$ = 12.5 Hz, $J$ = 3 Hz, H-3α), 6.08 (dd, 1H, $J$ = 4.5 Hz, $J$ = 2 Hz, H-9). HRMS(ESI+): calcd. for $C_{19}H_{30}O_5Na$ $[M+Na]^+$ 361.1991, found 361.1994; calcd. for $C_{15}H_{23}O$ $[M+H\text{-}2AcOH]^+$ 219.1749, found 219.1744; calcd. for $C_{15}H_{21}$ $[M+H\text{-}2AcOH\text{-}H_2O]^+$ 201.1643, found 201.1639; calcd. for $C_{12}H_{15}$ $[M+H\text{-}2AcOH\text{-}(CH_3)_2CO]^+$ 159.1174, found 159.1171.

### 4.9. Feeding experiments with labelled precursors

*B. cinerea* was grown at 25 °C on shake culture at 180 rpm in 500 ml Erlenmeyer flasks, each containing 200 ml of modified Czapek-Dox medium (30.0 g glucose, 1.0 g yeast extract, 1.0 g $KH_2PO_4$, 2.5 g $NaNO_3$, 0.5 g $MgSO_4$ $7H_2O$, 0.001 g $FeSO_4$ $7H_2O$, 0.5 g KCl, 0.005 g $CuSO_4$ $5H_2O$ and distilled water to 1.0 l). The pH of the medium was adjusted to 7.0 with an aq. soln. 1 M NaOH. Each flask was inoculated with $10^7$ fresh conidia coming from a 14–21 days old culture of *B. cinerea* on Tomato-Agar medium (0.5 l tomato juice, 20.0 g agar, and distilled water to 0.5 l).

After 5 days of incubation (see detailed experiments below) the mycelia was transferred into the same number of 500 ml Erlenmeyer flasks, each containing 200 ml of Czapek-Dox medium without glucose or with a reduced dose of glucose (15.0 g/l) and a filter-sterilized aq. soln. of the labelled precursor. Flasks were incubated under the same conditions described above for 3 days. Then, the culture medium and mycelia were separated by filtration. The broth was satd. with NaCl, and extracted with EtOAc (× 3). The EtOAc extract was washed with distilled $H_2O$ (× 3) and then dried over dry $Na_2SO_4$. The organic extract which was obtained, was evaporated at reduced pressure to dryness.

The extract was subjected to column chromatography on silica gel with an increasing gradient of EtOAc in *n*-hexane as eluent. Final purification was carried out by normal phase HPLC using a Lichrosfer Si 60 (10 μm) LichoCart (250 mm × 10 mm) column, *n*-hexane-EtOAc (25:75) as mobile phase and flow rate 2.5 ml/min to yield compound **11** ($t_R$. = 18 min).

#### 4.9.1. Feeding of sodium [1–$^{13}$C]-acetate to BcBOT2Δ

Twenty subcultured Erlenmeyer flasks with conidia of the *BcBOT2Δ* mutant (Pinedo et al., 2008) in Czapek-Dox medium with a reduced dose of glucose (15 g/l), were fed with a filter-sterilized soln. of sodium [1–$^{13}$C]-acetate in $H_2O$ on day 5 to a final concentration of 500 ppm. Extraction of the broth 3 days post-feeding yielded a extract (300.0 mg, 15 mg/bottle) which was purified as described above to afford **11** (2.3 mg).

#### 4.9.2. Feeding of sodium [2–$^{13}$C]-acetate to BcBOT2Δ

Fourteen Erlenmeyer flasks, each subcultured with $10^7$ fresh conidia in Czapek-Dox medium without glucose, were pulse fed on day 5 with an aseptic aq. soln. of sodium [2–$^{13}$C]-acetate to a final concentration of 500 ppm. Extraction of the broth 3 days post-feeding yielded a extract (50.0 mg, 3.6 mg/flask) which was purified as described in the general method to afford **11** (0.8 mg).

#### 4.9.3. Feeding of sodium [$^2H_3$]-acetate to BcBOT2Δ

In accordance with the above procedure, twenty subcultured Erlenmeyer flasks with conidia of *BcBOT2Δ* in Czapek-Dox medium without glucose, were pulse fed with a filter-sterilized soln. of sodium [$^2H_3$]-acetate in $H_2O$ on day 5 to a final concentration of 500 ppm. After 3 days post-feeding, the culture medium and mycelia were separated by filtration. Extraction of the broth yielded a eremophilenes extract (121.1 mg, 6.1 mg/flask), which was purified as described in the general method to afford the compound **11** (2.5 mg).

## Acknowledgments

This research was supported by grant from MINECO-FEDER (AGL2015-65684-C2-1-R) and CAPES-DGU collaborative grant between Brazil and Spain. Use of NMR facilities at the Servicio Centralizado de Ciencia y Tecnología (SCCYT) of the University of Cádiz is acknowledged.

## Appendix A. Supplementary data

Supplementary data related to this article can be found at http://dx.doi.org/10.1016/j.phytochem.2018.06.010.

## References

Amselem, J., Cuomo, C.A., van Kan, J.A.L., Viaud, M., Benito, E.P., Couloux, A., Coutinho, P.M., de Vries, R.P., Dyer, P.S., Fillinger, S., Fournier, E., Gout, L., Hahn, M., Kohn, L., Lapalu, N., Plummer, K.M., Pradier, J.-M., Quévillon, E., Sharon, A., Simon, A., ten Have, A., Tudzynski, B., Tudzynski, P., Wincker, P., Andrew, M., Anthouard, V., Beever, R.E., Beffa, R., Benoit, I., Bouzid, O., Brault, B., Chen, Z., Choquer, M., Collémare, J., Cotton, P., Danchin, E.G., Da Silva, C., Gautier, A., Giraud, C., Giraud, T., Gonzalez, C., Grossetete, S., Güldener, U., Henrissat, B., Howlett, B.J., Kodira, C., Kretschmer, M., Lappartient, A., Leroch, M., Levis, C., Mauceli, E., Neuvéglise, C., Oeser, B., Pearson, M., Poulain, J., Poussereau, N., Quesneville, H., Rascle, C., Schumacher, J., Ségurens, B., Sexton, A., Silva, E., Sirven, C., Soanes, D.M., Talbot, N.J., Templeton, M., Yandava, C., Yarden, O., Zeng, Q., Rollins, J.A., Lebrun, M.-H., Dickman, M., 2011. Genomic analysis of the necrotrophic fungal pathogens Sclerotinia sclerotiorum and Botrytis cinerea. PLoS Genet. 7, e1002230. https://doi.org/10.1371/journal.pgen.1002230.

Baker, R., Coles, H.R., Edwards, M., Evans, D.A., Howse, P.E., Walmsley, S., 1981. Chemical composition of the frontal gland secretion of *Syntermes soldiers* (*Isoptera*, *Termitidae*). J. Chem. Ecol. 7, 135–145. https://doi.org/10.1007/BF00988641.

Blay, G., Bargues, V., Cardona, L., García, B., Pedro, J.R., 2001. Ultrasound assisted reductive cleavage of eudesmane and guaiane γ-enonelactones. Synthesis of 1α,7α,10αH-guaian-4,11-dien-3-one and hydrocolorenone from santonin. Tetrahedron 57, 9719–9725. https://doi.org/10.1016/S0040-4020(01)00986-3.

Botubol, J.M., Durán-Peña, M.J., Macías-Sánchez, A.J., Hanson, J.R., Collado, I.G., Hernández-Galán, R., 2014. The asymmetric total synthesis of cinbotolide: a revision of the original structure. J. Org. Chem. 79, 11349–11358. https://doi.org/10.1021/jo501471m.

Cane, D.E., Rawlings, B.J., Yang, C.-C., 1987. Isolation of (-)-γ-cadinene and aristolochene from *Aspergillus terreus*. J. Antibiot. (Tokyo) 40, 1331–1334. https://doi.org/10.7164/antibiotics.40.1331.

Collado, I.G., Viaud, M., 2016. Secondary metabolism in Botrytis cinerea: combining genomic and metabolomic approaches. In: Botrytis – the Fungus, the Pathogen and its Management in Agricultural Systems. Springer International Publishing, Cham, pp. 291–313. https://doi.org/10.1007/978-3-319-23371-0_15.

Colmenares, A.J., Aleu, J., Durán-Patrón, R., Collado, I.G., Hernández-Galán, R., 2002. The putative role of botrydial and related metabolites in the infection mechanism of *Botrytis cinerea*. J. Chem. Ecol. 28, 997–1005.

Dalmais, B., Schumacher, J., Moraga, J., Le Pecheur, P., Tudzynski, B., Collado, I.G., Viaud, M., 2011. The *Botrytis cinerea* phytotoxin botcinic acid requires two polyketide synthases for production and has a redundant role in virulence with botrydial. Mol. Plant Pathol. 12, 564–579. https://doi.org/10.1111/j.1364-3703.2010.00692.x.

Dean, R., van Kan, J.A.L., Pretorius, Z.A., Hammond-Kosack, K.E., Di Pietro, A., Spanu, P.D., Rudd, J.J., Dickman, M., Kahmann, R., Ellis, J., Foster, G.D., 2012. The top 10 fungal pathogens in molecular plant pathology. Mol. Plant Pathol. 13, 414–430.

https://doi.org/10.1111/j.1364-3703.2011.00783.x.
Elad, Y., Pertot, I., Cotes Prado, A.M., Stewart, A., 2016. Plant hosts of *Botrytis* spp. In: Botrytis – the Fungus, the Pathogen and its Management in Agricultural Systems. Springer International Publishing, Cham, pp. 413–486. https://doi.org/10.1007/978-3-319-23371-0_20.
Faraldos, J.A., Wu, S., Chappell, J., Coates, R.M., 2007. Conformational analysis of (+)-germacrene A by variable temperature NMR and NOE spectroscopy. Tetrahedron 63, 7733–7742. https://doi.org/10.1016/j.tet.2007.04.037.
Faraldos, J.A., Kariuki, B., Allemann, R.K., 2010. Intermediacy of eudesmane cation during catalysis by aristolochene synthase. J. Org. Chem. 75, 1119–1125. https://doi.org/10.1021/jo902397v.
González, C., Brito, N., Sharon, A., 2016. Infection process and fungal virulence factors. In: Botrytis – the Fungus, the Pathogen and its Management in Agricultural Systems. Springer International Publishing, Cham, pp. 229–246. https://doi.org/10.1007/978-3-319-23371-0_12.
Govindachari, T.R., Mohamed, P.A., Parthasarathy, P.C., 1970. Ishwarane and aristolochene, two new sesquiterpene hydrocarbons from *Aristolochia indica*. Tetrahedron 26, 615–619. https://doi.org/10.1016/S0040-4020(01)97854-8.
Maffei, M.E., Arimura, G.-I., Mithöfer, A., 2012. Natural elicitors, effectors and modulators of plant responses. Nat. Prod. Rep. 29, 1288–1303. https://doi.org/10.1039/c2np20053h.
Marumo, S., Katayama, M., Komori, E., Ozaki, Y., Natsumeand, M., Kondo, S., 1982. Microbial production of abscisic acid by *Botrytis cinerea*. Agric. Biol. Chem. 46, 1967–1968.
Oliva, R., Win, J., Raffaele, S., Boutemy, L., Bozkurt, T.O., Chaparro-Garcia, A., Segretin, M.E., Stam, R., Schornack, S., Cano, L.M., Van Damme, M., Huitema, E., Thines, M., Banfield, M.J., Kamoun, S., 2010. Recent developments in effector biology of filamentous plant pathogens. Cell. Microbiol. 12, 705–715. https://doi.org/10.1111/j.1462-5822.2010.01471.x.
Pinedo, C., Wang, C.-M., Pradier, J.-M., Dalmais, B., Choquer, M., Le Pêcheur, P., Morgant, G., Collado, I.G., Cane, D.E., Viaud, M., 2008. Sesquiterpene synthase from the botrydial biosynthetic gene cluster of the phytopathogen *Botrytis cinerea*. ACS Chem. Biol. 3, 791–801. https://doi.org/10.1021/cb800225v.
Pinedo, C., Moraga, J., Barúa, J., González-Rodríguez, V.E., Aleu, J., Durán-Patrón, R., Macías-Sánchez, A.J., Hanson, J.R., Viaud, M., Hernández-Galán, R., Garrido, C., Collado, I.G., 2016. Chemically induced cryptic sesquiterpenoids and expression of sesquiterpene cyclases in *Botrytis cinerea* revealed new sporogenic (+)-4-epi*er*-emophil-9-en-11-ols. ACS Chem. Biol. 11, 1391–1400. https://doi.org/10.1021/acschembio.5b00931.
Quidde, T., Osbourn, A., Tudzynski, P., 1998. Detoxification of α-tomatine by *Botrytis cinerea*. Physiol. Mol. Plant Pathol. 52, 151–165. https://doi.org/10.1006/PMPP.1998.0142.
Scherlach, K., Hertweck, C., 2009. Triggering cryptic natural product biosynthesis in microorganisms. Org. Biomol. Chem. 7, 1753–1760. https://doi.org/10.1039/b821578b.
Tani, H., Koshino, H., Sakuno, E., Nakajima, H., 2005. Botcinins A, B, C, and D, metabolites produced by *Botrytis cinerea*, and their antifungal activity against *Magnaporthe grisea*, a pathogen of rice blast disease. J. Nat. Prod. 68, 1768–1772. https://doi.org/10.1021/NP0503855.
Tani, H., Koshino, H., Sakuno, E., Cutler, H.G., Nakajima, H., 2006. Botcinins E and F and botcinolide from *Botrytis cinerea* and structural revision of botcinolides. J. Nat. Prod. 69 755–725. https://doi.org/10.1021/NP060071X.
Terada, Y., Yamamura, S., 1979. Stereochemical studies on germacrenes: an application of molecular mechanics calculations. Tetrahedron Lett. 20, 3303–3306. https://doi.org/10.1016/S0040-4039(01)95391-2.
van Kan, J.A.L., 2006. Licensed to kill: the lifestyle of a necrotrophic plant pathogen. Trends Plant Sci. 11, 247–253. https://doi.org/10.1016/j.tplants.2006.03.005.
van Kan, J.A.L., Shaw, M.W., Grant-Downton, R.T., 2014. Botrytis species: relentless necrotrophic thugs or endophytes gone rogue? Mol. Plant Pathol. 15, 957–961. https://doi.org/10.1111/mpp.12148.
Wharton, P.S., Poon, Y.-C., Kluender, H.C., 1973. Conformational isomerism in dihydropregeijerene and hedycaryol. J. Org. Chem. 38, 735–740. https://doi.org/10.1021/jo00944a025.
Whiteheah, I.M., Threlfall, D.R., Ewing, D.F., 1987. Cis-9,10-dihydrocapsenone: a possible catabolite of capsidiol from cell suspension cultures of *Capsicum annuum*. Phytochemistry 26, 1367–1369. https://doi.org/10.1016/S0031-9422(00)81814-2.
Williamson, B., Tudzynski, B., Tudzynski, P., van Kan, J.A.L., 2007. Botrytis cinerea: the cause of grey mould disease. Mol. Plant Pathol. 8, 561–580. https://doi.org/10.1111/j.1364-3703.2007.00417.x.
Zhao, Y., Schenk, D.J., Takahashi, S., Chappell, J., Coates, R.M., 2004. Eremophilane sesquiterpenes from capsidiol. J. Org. Chem. 69, 7428–7435. https://doi.org/10.1021/JO049058C.
Ōsawa, E., Shimada, K., Kodama, M., Itô, S., 1979. Conformation of hedycaryol isomers. Tetrahedron Lett. 20, 2353–2354. https://doi.org/10.1016/S0040-4039(01)93971-1.